From *Journal of Advanced Robotics*, 11(4), December 1997, pp 341-358.

Rocky 7: A Next Generation Mars Rover Prototype

Richard Volpe, J. Balaram, Timothy Ohm, and Robert Ivlev
Jet Propulsion Laboratory
California Institute of Technology
Pasadena, California 91109

Abstract

This paper provides a system overview of a new Mars rover prototype, Rocky 7[1]. We describe all system aspects: mechanical and electrical design, computer and software infrastructure, algorithms for navigation and manipulation, science data acquisition, and outdoor rover testing. In each area, the improved or added functionality is explained in a context of its path to flight, and within the constraints of desired science missions.

1 Introduction

In 1996, NASA launched the first of a series of spacecraft to revisit the planet Mars. This *Pathfinder*[2] lander contains the 'Sojourner' microrover flight experiment, an 11.5 kg six-wheeled mobile robot which will venture out from the lander, taking pictures and positioning a science instrument against designated soil and rocks.

Subsequent to this mission, there are plans to return to the surface of Mars every 26 months through 2005. It is anticipated that Sojourner will demonstrate the viability of mobile robot exploration of Mars, and longer range surface traversals with more instrumentation will be desirable in the follow-on missions. Therefore, we are investigating next generation rovers with more mobility, autonomy, and functionality.

Recently we have completed construction and demonstration of a new prototype, Rocky 7, as shown in Figure 1. Compared to its predecessors, this microrover features [6]:

- Modern computer system with real-time operating system
- Reconfigurable software development environment
- Bi-directional stereo vision navigation
- Mini-manipulator for sample acquisition and pointing of integrated science instruments
- Less locomotion actuators for mass and complexity reduction
- Pointable solar array for greater power collection
- Comparable low mass and size

[1] http://robotics.jpl.nasa.gov/tasks/scirover/
[2] http://mpfwww.jpl.nasa.gov/

This paper provides a system overview of Rocky 7 and gives details on each of the advances it includes. In Section 2 we describe specifications and construction of the vehicle and its manipulator. Section 3 provides a similar level of detail describing the constituent computer, sensors, actuators, and custom electronics. The software architecture and algorithms for navigation, manipulation, and vision, are presented in Section 4. In Section 5, we discuss the science data gathering capabilities of the rover, and present some measurements obtained with it. Finally, Section 6 describes our construction of a Mars-like outdoor test area, and initial rover test conducted in it.

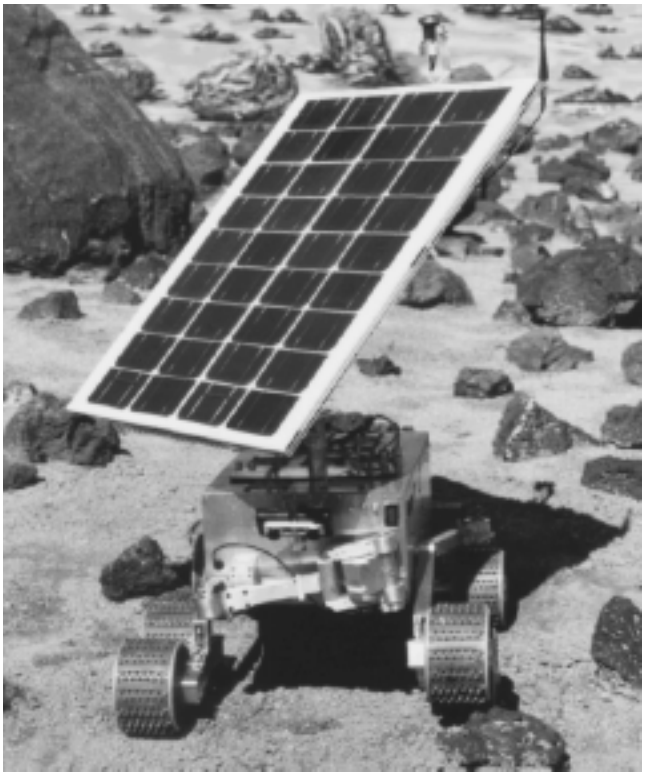

Figure 1: *Rocky 7.*

Dimensions (cm)	$61 \times 49 \times 31$
wheel diameter	13
chassis volume	$41 \times 27 \times 15$
arm reach	33
ground clearance	16
Mass Total (kg)	**11.5**
sensors	1
computer system	2.5
motors	2
structure	4
batteries	2
solar panel (optional)	2
Power Requirements (W)	**48**
computer system	28
sensors	6
motors (nominal)	8
power conditioning	6
Max Speed (cm/s)	**30**

Table 1: *Rocky 7 specifications.*

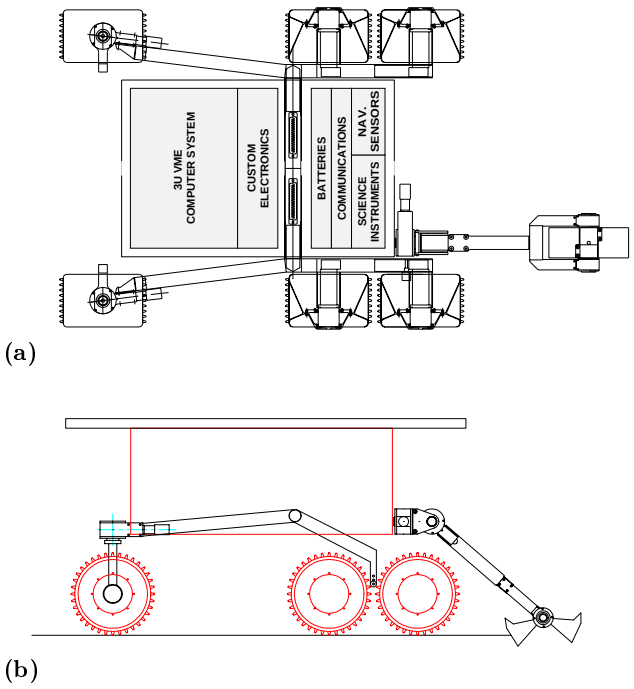

(a)

(b)

Figure 2: *Rocky 7 top and side views.*

2 Mechanical Design

As shown in Table 1, Rocky 7 is approximately the same size and mass as Sojourner. It also has the same number of degrees-of-freedom (DOFs), but with more functionality. Figures 2 (a) and (b) show how this is accomplished by a new wheel configuration, and an integrated mini-manipulator.

Like Sojourner Rocky 7 employs a *rocker-bogie* six wheel configuration [2]. However, unlike its predecessors with four corner steering, Rocky 7 only has steering capability on two corners, driving like a car or fork-lift. Also, the wheels on each rocker have been moved close together. While not greatly reducing its step climbing capability (approximately 1.5 wheel diameters), this configuration creates the possibility of mechanically or electrically controlling these two wheels together. In this way, the number of DOFs for mobility has been reduced from ten to six. The cost of this change is an inability to turn in place about the center of the vehicle, as with four corner steering. Instead, the nominal rotation axis for Rocky 7 is located mid-way between the double wheel pairs. (Tank steering can be used to approximate turn in place operations, but the extensive wheel slippage corrupts odometer information, and causes the vehicle to sink into soft soils like those expected on Mars.)

The four DOFs saved with the new wheel configuration have been used for a manipulator that can sample soil or rocks, and point or bury science instruments. This small arm has a two DOF shoulder that can store it across the front of the chassis, reach down to 10 cm below the surface, or move in a conical fashion in front of the vehicle to point an integrated spectrometer. The end-effector of the arm has two independently drivable scoops, which can rotate continuously. In this way, they can be positioned as a clamshell to scoop and store soil samples, or back to back to form a parallel jaw gripper with side tongs allowing rock and cylindrical instrument grasping. Also, when rotated together through 360°, they deploy a white target stored in the fork of the end effector. This target is used for calibrating a built-in spectrometer.

Figure 10 shows how the optical path for this point spectrometer is integrated into the end-effector. One scoop rotates on a hub that is partially recessed inside the hub of the other scoop. Each hub has a small hole in it. For one relative angle between the scoops, the holes align and open an aperture. Inside the hub of the scoops, is a mirror at 45° tilt, deflecting the light to another mirror at one end of the rotation axis of the scoops. This second mirror deflects light into a fiber, and back to a spectrometer in the chassis.

The spectrometer light path, as well as motor wiring without service loops, is enabled by a new joint design created for Rocky 7 [10]. In addition to having a cylindrical opening along the axis of rotation, this design is a non-backdrivable, high torque, right angle gearbox. It has been used on all four arm joints, as well as the two steering joints of the vehicle.

The last DOF of Rocky 7 can be used for pointable solar panel. Instead of the flat, fixed solar panel used by Sojourner, Rocky 7 employs a version which is tilted to the average sun angle in the sky. In medium to high latitude missions with clear skies, a rover on Mars will need to track the sun to absorb more light by its solar panel. We utilize a single DOF panel to demonstrate this capability with minimal added complexity to the system.

Item	Vendor	Model	Comment
CPU	OR	VPU-40	33MHz 16MB
A/D conv.	OR	VADC-20	32 chan.
Digital I/O	OR	VPAR10	
Ethernet	Dynatem	DLAN	
Adaptor	Dynatem	DPC104	3UVME/PC104
Framegrab	ImageNation	CX104	2, B/W
Backplane	TreNew	J1BUS	7 slot 3UVME

Table 2: *Rocky 7 computer system.*

Item	Vendor	Model	Comment
Camera	Super Circuits	PC-8P	4, 120° fov
Accelerometer	Lucas Schaevitz	LSMP-2	3, $\pm 2g$
Angular Rate	Systron Donner	QRS11	$\pm 100°/s$
Sun Position	Lockheed Martin	WASS	prototype
Spectrometer	Ocean Optics	S1000	360-850 nm
Laser Pointer	SDL	7432-P2	680 nm
Motor/Enc	Maxon	RE025	6, wheels
Motor/Enc	MicroMo	1219,1331	4, arm/steer
Fan	Micronel	F62LM00	9

Table 3: *Rocky 7 actuators and sensors.*

Item	Vendor	Model	Comment
Motor Control	National	LM629	13 used
H-Bridge	Unitrode	L298D	7 dual
Video Select	Maxim	MAX454	dual 4 chan.
DC/DC conv	Comp Prod	various	$\pm 12, \pm 5, \pm 15$V
Batteries	Panasonic	P-120AS	4/5Af NiCad

Table 4: *Rocky 7 custom electronics.*

3 Electrical Design

The internal arrangement of the electrical subsystems of Rocky 7 is shown in Figure 2 (a). The components of the computer system, navigation sensors, and custom electronics are detailed in Tables 2, 3, and 4. Their power requirements are outlined in Table 1. It is apparent that the computer system is the largest user of power and space. The selection of this system was governed the desire for speed in both development and experimentation with the rover. For development purposes we desired commercial off-the-shelf (COTS) hardware, and a commercial hard-real-time operating system (Wind River Systems' $VxWorks^{TM}$). Both have a direct path to flight in a new low power/volume/mass Advanced Flight Computer (AFC) system being developed at JPL [1]. For experimentation, higher computation rates (and thus greater power consumption) are desirable to enable more efficient use of the researchers' time.

The sensor suite of Rocky 7 is a superset of those on Sojourner. The accelerometer and angular rate sensors are exact copies. The motor encoders are similar. The CCD cameras are COTS products, instead of the custom ones used on Sojourner. These items also have a new flight counterpart that is under development for future missions — the Active Pixel Sensor [5]. Similarly, the spectrometer is an COTS instrument integrated for demonstration purposes. Flight counterparts are being developed by several scientific teams interested in participating in future missions. The sun position sensor is a prototype that has been developed for Rocky 7 by *Lockheed Martin*. Its addition provides a new capability for Mars microrovers: absolute heading measurement, replacing the estimation nominally done via integration of the angular rate sensor signal.

Rocky 7's custom electronics perform power distribution and conversion, motor control, and video signal selection. The power conversion components are COTS and have flight counterparts. The variable speed motor controllers provide an improvement over the switched power bang-bang control used by Sojourner. For example, Rocky 7 can move any increment in distance and turn without slippage about any radius. Potential flight use of these COTS motor controllers is being explored, as well as functional replacement of them by Field Programmable Gate Arrays (FPGA) available on the AFC. Video selection circuitry is required on Rocky 7 because of the multiple sets of analog stereo cameras, but will not be needed with digital APS-based cameras. Finally, rechargeable COTS NiCad batteries are used to supplement or fully replace solar power on Rocky 7, due to dependability and the extra power requirements of the computer system.

4 Software

4.1 Architecture

Rocky 7's software architecture is based on the framework provided by Real Time Innovation's $ControlShell^{TM}$ and $NDDS^{TM}$ [11]. *Control Shell* facilitates the creation of C++ software modules which are connected into asynchronous finite state machines, and synchronous data-flow control loops. *NDDS* is a Network Data Delivery System, which enables communications between *Control Shell* processes, as well as separate user applications.

In Rocky 7, asynchronous activities are initiated by a queue of operator commands. On-board the rover, these commands cause state transitions in one of three state machines: Navigation, Vision, and Manipulation. For example, Figure 3 shows the Navigation state machine. Each state transition runs the execution method in the C++ object labeling the transition arrow. State machine transitions are often used to begin the execution of synchronous processes which perform monitoring and control of the Rover's subsystems. For instance, Figure 4 shows a data flow graph used to configure Rocky 7 for measuring the vehicle state.

4.2 Operator Interface

GCTL, our "ground control" operator interface software, enables the creation of a task queue for the rover, and sends the commands one at a time as each previous command is completed successfully. While commands exist for activities of manipulation and vision, typical task queues consist

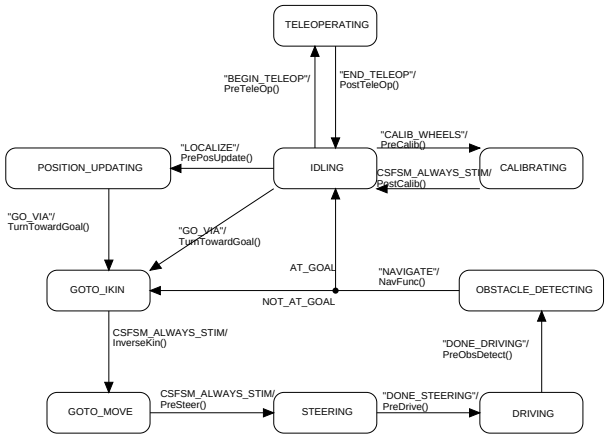

Figure 3: *Rocky 7 "Navigation" state machine.*

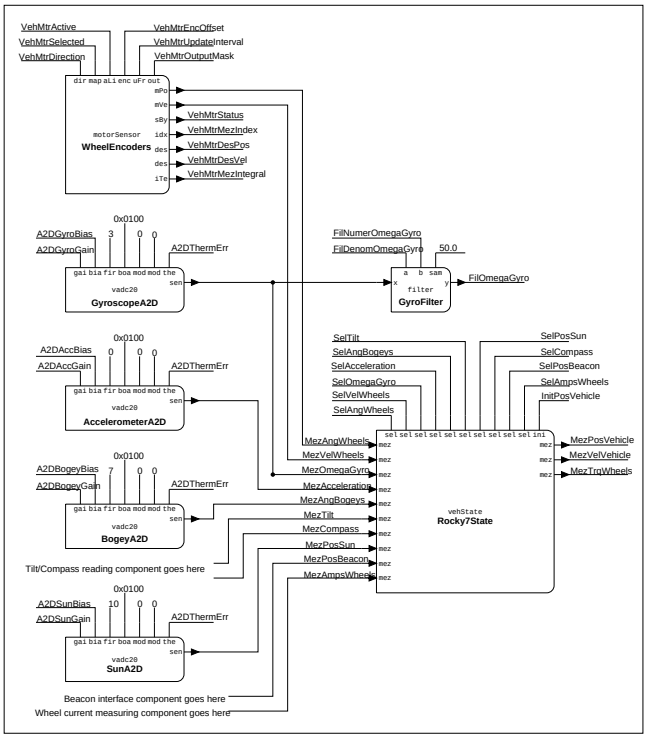

Figure 4: *Rocky 7 "Vehicle State" data flow graph.*

largely of way-point commands for navigation. To create a list of way-points, a graphical user interface enables the user to select three dimensional points via interactive stereo correlation of a pair of lander images, as shown Figure 5.

4.3 Navigation

One at a time, way-points are provided to Rocky 7, which employs the Rocky 3 navigation algorithm to navigate to the desired location [7]. This algorithm is outlined in Figure 6. The current parameter values for this algorithm are given

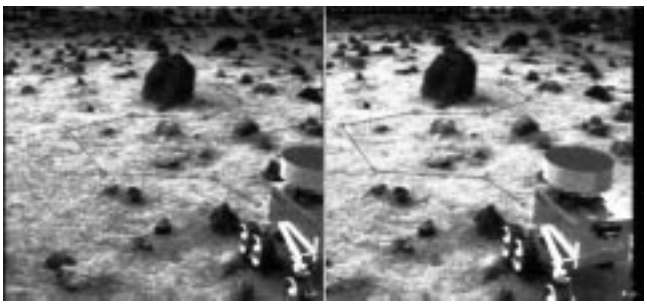

Figure 5: *Selecting way-points with GCTL.*

Parameter	Value	
nominal translation	0.25	m
nominal rotation	0.5	rad
small orientation error	$0.0 \leq 0.2$	rad
medium orientation error	$0.2 \leq 1.0$	rad
large orientation error	> 1.0	rad
small position error	$0.0 \leq 0.25$	m
medium position error	$0.25 \leq 1.5$	m
large position error	> 1.5	m

Table 5: *Rocky 7 navigation parameters.*

in Table 5.

Step 1, localization, is necessary to update the rover's sense of its position in the environment around the lander. This value can accumulate error in between updates due to wheel slippage and angular rate sensor drift. Whereas Sojourner employs manual estimation of the rover's position and orientation by an Earth-based operator, we employ *automatic* localization by viewing a colored-cylinder on Rocky 7 [12]. Further, to enable operations outside of view of the lander and allow the use of the pointable solar panel, we are upgrading the localization method to obtain the position and orientation of the rover from a radio beacon and sun sensor.

Steps 2 and 3 are self-explanatory. Step 4, is described in the next section.

Step 5, describes how the rover will incrementally turn in place searching for a clear path, after having encountered an obstacle. A clear path is defined as an obstacle free path wider than the turning circle of the vehicle. However, in some terrains, this definition can be over restrictive. Figure 7 (a) illustrates the situation of two obstacles between which the vehicle can drive, although they are within the turning circle. The rover is the rectangle, the circle is its turning envelope, and the triangle is its sensing envelope. In its initial orientation (solid lines), the rover will detect an obstacle in the left shaded region. It then turns incrementally right (dashed lines) and detects another obstacle in the right shaded region. In this case, the rover will remember its current state, turn halfway back to the left attempting to "thread the needle".

Step 6 describes the procedure for threading the needle.

```
1. LOCALIZATION
   measure global rover position from lander
2. WAY-POINT
   set new reference position from task queue
3. TURN-TO-GOAL
   if position error is small
     goto 1
   else
     turn in place toward goal
4. OBSTACLE-DETECT
   measure terrain in front of rover
5. TURN-IN-PLACE
   if obstacles center or left and right
         turn nominal rotation right
  goto 4
   if obstacles left/right
      if previous obstacle right/left
          turn half nominal rotation right/left
          goto 6
      else
          turn nominal rotation right/left
          goto 4
6. THREAD-THE-NEEDLE
   if obstacles center
     move total alley length straight backward
     goto 4
   else if obstacles left or right
     move nominal translation straight forward
     increment total alley length
     obstacle_detect
     goto 6
   else if obstacles clear
     move nominal translation straight forward
     goto 4
7. LOOP-TO-GOAL
   if orientation error is small
      move nominal translation straight forward
   else if orientation error is medium
      set turn radius to large
      move nominal translation forward
   else if orientation error is large
      if position error is medium
        goto 3
      else
        set turn radius to small
        move nominal translation forward
   goto 4
```

Figure 6: Rocky 3 navigation algorithm.

The main concern in this procedure is that the rover will enter a dead-end alley. Since the rover is considered to be in the alley as long as obstacles remain to the immediate left or right, the turn in place procedure is not possible. Therefore, if an obstacle is eventually detected straight ahead, the rover retreats the entire remembered length of the alley and resumes its original turn in place operations from Step 5, also remembering how far it had turned and in which direction.

Step 7, loop to the goal, governs the steering of the rover when clear of obstacles. After clearing an obstacle, the rover does not turn to face the goal, but rather moves in an arc toward it. This prevents the situation of turning away from an obstacle in an avoidance move, and then turning back toward it in an attempt to drive to the goal. The radius of the arc is governed by the heading error of the rover, as shown in Figure 7 (b): a small radius arc for large error, large radius for medium error, and no turn for small error. However, for some distances to the goal the smallest radius arc may not be small enough, and the rover will begin to orbit the goal. To prevent this, the rover will turn to face the goal when within a medium distance error from it.

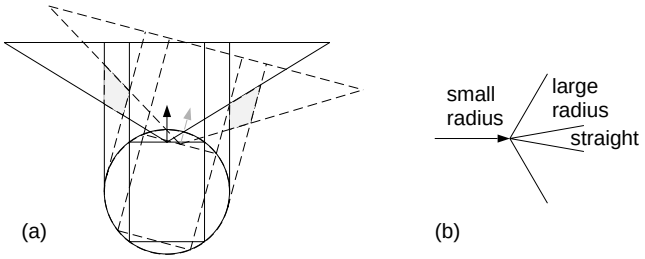

Figure 7: *Rocky 7 navigation: (a) threading the needle, (b) loop to goal.*

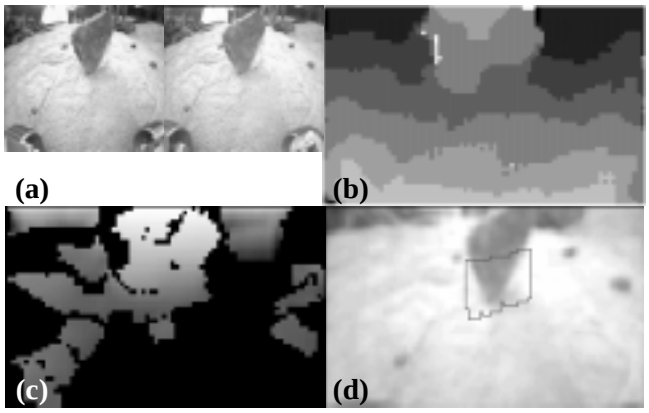

Figure 8: *Rocky 7 stereo vision processing step results: (a) image pair (b) disparity, (c) elevation map, (d) obstacle detection.*

4.4 Stereo Vision

Rocky 7 has camera pairs with 5 cm baselines at both ends of the vehicle, enabling bi-directional driving with stereo vision obstacle avoidance. Figure 8 shows the processing steps of this strategy [8].

The image pair in Figure 8(a) shows a rock field with a prominent obstacle in front of the rover. Using a camera model developed by off-line calibration, these images are warped to remove the radial distortion. The resulting rectified images are suitable for further processing for obstacle detection.

Pyramid image processing results in left and right band-pass filtered, low-resolution images. Using these processed

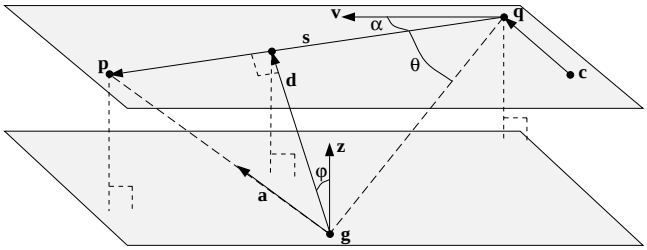

Figure 9: *Rocky 7 manipulation geometry.*

image pairs, Figure 8(b) shows the integer value disparities computed using a correlation window. Subpixel disparities are then computed for high-confidence disparity values and processed using the camera model to get the elevation map in Figure 8(c). Bright areas indicate high spots, dark areas indicate low areas or low-confidence regions.

The elevation map is analyzed for abrupt changes in height or high-centering hazards. Figure 8(d) indicates a region where the rover is not able to traverse. The final result of the processing is passed to the navigation algorithm as a fuzzy classification of the region position: left, right, or center. As indicated previously by Figure 6, the central region is defined as the width of the vehicle extending out to 50 cm. The left and right regions are from either side of the central region to the edge of the field of view.

4.5 Kinematic Models

To move Rocky 7, we model the rover as a planar four wheel vehicle, ignoring rocker-bogie positions. Then, the kinematics for Ackerman steering are employed [4]. Driving with the steering wheels in the front or rear is allowed.

For manipulation the kinematics are described by Figure 9: The vehicle center is at $\mathbf{c}$, facing direction $\mathbf{v}$ with $\mathbf{z}$ up. The goal point and approach vector are given as $\mathbf{g}$ and $\mathbf{a}$. It is necessary to solve for the required rotation and displacement of the vehicle, α and x, and the arm angles $\theta = [\varphi, \theta, \sigma]^T$.

The approach position is at $\mathbf{p}$ along a vector $\mathbf{s}$ from the shoulder:

$$\mathbf{p} = \mathbf{g} + \hat{\mathbf{a}} \left[\frac{(\mathbf{q} - \mathbf{g}) \cdot \hat{\mathbf{z}}}{\hat{\mathbf{a}} \cdot \hat{\mathbf{z}}} \right] \quad (1)$$

$$\mathbf{s} = \mathbf{q} - \mathbf{p} \quad (2)$$

Due to its limited degrees of freedom, the arm must be aligned within the plane containing $\mathbf{s}$ and $\mathbf{g}$, by rotating and translating the rover (generating only rotation about point $\mathbf{q}$):

$$\alpha = \cos^{-1}(\hat{\mathbf{v}} \cdot \hat{\mathbf{s}}) \quad (3)$$

$$x = |\mathbf{c} - \mathbf{q}|\alpha \quad (4)$$

The unit vector in the direction of the projection of the goal point onto $\mathbf{s}$ is:

$$\hat{\mathbf{d}} = \hat{\mathbf{s}} \times (\hat{\mathbf{s}} \times \hat{\mathbf{a}}) \quad (5)$$

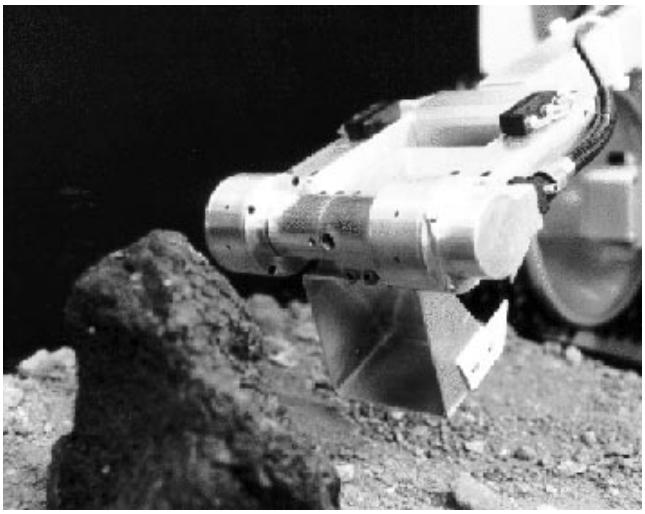

Figure 10: *Rocky 7 spectrometer pointing.*

To orient the arm of length L in the plane of the approach vector and reach the goal, the desired angles of the two shoulder joints are:

$$\varphi = \sin^{-1}\left(|\hat{\mathbf{z}} \times \hat{\mathbf{d}}|\right) \quad (6)$$

$$\theta = \sin^{-1}\left[\frac{(\mathbf{p} - \mathbf{g}) \cdot \hat{\mathbf{d}}}{L}\right] \quad (7)$$

Therefore, the alignment of the scoops along the approach vector is:

$$\sigma = \cos^{-1}(\hat{\mathbf{a}} \cdot \hat{\mathbf{s}}) - \theta \quad (8)$$

It is also necessary to move the vehicle to bring the goal within reach:

$$x = L\cos\theta - |\mathbf{g} + \mathbf{d} - \mathbf{q}| \quad (9)$$

5 Science Mission

The primary purpose of a Mars Rover is to provide access to science targets on the surface, such as rocks and soil. Therefore, we attempt to treat the integration and use of science instruments as equally important as enabling technologies like mobility and manipulation. Initially, three science enabling capabilities have been considered: spectrographic pointing measurement, seismometer burial, and close-up imaging.

As described in Section 2, Rocky 7 has an Ocean Optics point spectrometer (sensitive from 350-800 nm) which can be aimed by its manipulator, as shown in Figure 10. We have used this spectrometer to measure and automatically match spectra from a set of geologically interesting rock types. Figure 11 shows the data for some of these tests.

Seismometer burial is desirable to provide good acoustic coupling with the planet, and to filter wind noise. Proposed micro-seismometers for Mars are housed in 5 cm diameter cylindrical vessels, which can be grasped by the tongs on

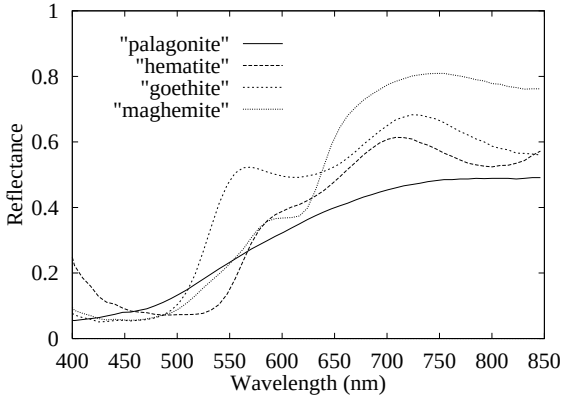

Figure 11: *Spectra for several Mars-like substances.*

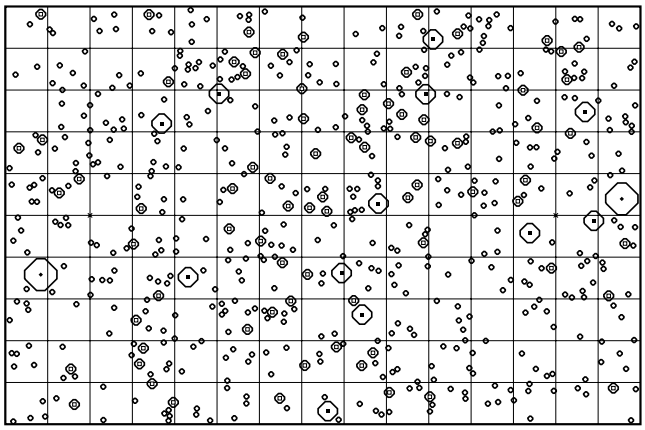

Figure 12: *Rock distribution map for Mars nominal terrain.*

Rocky 7's end-effector [3]. As illustrated by Figure 2(b), Rocky 7's manipulator can dig a hole as deep as 10 cm, in which such a seismometer can be buried. Development of algorithms to perform these actions is in progress.

Finally, we have directly extended the navigation imaging for scientific use. Close-up, full resolution images, may be obtained at designated way-points, as well as during other operations such as digging. We are also integrating a laser that will shine down the optical path of the spectrometer and illuminate the surface before a spectrometer reading. This laser spot can then be imaged, providing a record of the exact location of a surface that was spectrographically measured, giving more context to the data.

6 Outdoor Testing

To test Rocky 7 in a realistic environment, we have built the *MarsYard*, a 15×25 meter outdoor test area that replicates the rock frequency distribution for three terrain types categorized by Viking Mission data: Mars nominal, Viking Lander 1, Viking Lander 2 [9]. Figure 12 shows the least dense of these terrains, Mars nominal. Each grid cell is one meter square, and the icons represent the locations of rocks of sizes 0-7.5 cm, 7.5-15 cm, 15-30 cm, and 30-60 cm.

As shown previously in Figure 5, all initial tests were conducted in this terrain. A typical test scenario involved the acquisition of set of lander images, specification by the operator of a series of 5-10 way-points with several spectrometer pointing operations interspersed. The last spectrometer reading was typically followed by a dig operation. Upon return to the lander, the soil was dumped, to demonstrate a sample return scenario. Future tests will extend this functionality to non-line of sight traversals with more science operations, as discussed earlier.

7 Summary

This paper has provided an overview of the newly developed Rocky 7 Mars rover prototype. All aspects of the system have been discussed: mechanical, electrical, computer, software, algorithms, science instruments, and initial tests. We have also described how this system demonstrates improvements over its predecessors, and provides a viable path to flight for upcoming missions in the next 10 years.

8 Acknowledgments

This work has involved the efforts of many people whom we would like to thank: Don Bickler, Johnathan Cameron, Veronica Gauss, Samad Hayati, Geoff Harvey, Todd Litwin, Larry Matthies, Steve Peters, Rob Steele, Susan Ung, James Wang, Rick Welch, and Brian Wilcox.

The research described in this paper was carried out by the Jet Propulsion Laboratory, California Institute of Technology, under a contract with the National Aeronautics and Space Administration. Reference herein to any specific commercial product, process, or service by trade name, trademark, manufacturer, or otherwise, does not constitute or imply its endorsement by the United States Government or the Jet Propulsion Laboratory, California Institute of Technology.

References

[1] L. Alkalai and B. Jarvis. The Design and Implementation of NASA's Advanced Flight Computing Module. In *Proceedings of the IEEE MCM Conference*, Santa Cruz, CA, Jan. 31 – Feb. 2 1995.

[2] D. Bickler. A New Family of JPL Planetary Surface Vehicles. In *Missions, Technologies, and Design of Planetary Mobile Vehicles*, pages 301–306, Toulouse, France, September 28-30 1992.

[3] C. Budney et al. SEI Science Payloads: Descriptions and Delivery Requirements. Technical Report D-7955

(internal document), Jet Propulsion Laboratory, California Institute of Technology, Pasadena, CA, May 1991.

[4] L. Feng, J. Borenstein, and H. Everett. "Where am I?": Sensors and Methods for Autonomous Mobile Robot Positioning. Technical Report UM-MEAM-94-21, University of Michigan, Ann Arbor, MI, December 1994.

[5] E. Fossum, S. Mendis, and B. Pain. Active-Pixel Image Sensor with Analog-to-Digital Converters. Technical Support Package NPO-19117 (internal document), Jet Propulsion Laboratory, California Institute of Technology, Pasadena, CA, July 1995.

[6] E. Gat et al. Behavior Control for Robotic Exploration of Planetary Surfaces. *IEEE Transactions on Robotics and Automation*, 10(4):490–503, 1994.

[7] L. Matthies et al. Mars Microrover Navigation: Performance Evaluation and Enhancement. In *IEEE/RSJ International Conference on Robots and Systems (IROS)*, Pittsburgh, PA, August 5-9 1995.

[8] L. Matthies and P. Grandjean. Stochastic Performance Modeling and Evaluation of Obstacle Detectability with Imaging Range Sensors. *IEEE Transactions on Robotics and Automation*, 10(6):783–791, December 1994.

[9] H. Moore and B. Jakosky. Viking landing sites, remote-sensing observations, and physical properties of Martian surface materials. *Icarus*, 81:164–184, 1989.

[10] T. Ohm. High Torque Right Angle Gearbox Concept. Technical Support Package NPO-19542 (internal document), Jet Propulsion Laboratory, California Institute of Technology, Pasadena, CA, January 1995.

[11] S. Schneider, V. Chen, and G. Pardo-Castellote. ControllShell: A Real-Time Software Framework. In *AIAA Conference on Intelligent Robots in Field, Factory, Service, and Space (CIRFFSS)*, Houston, Texas, March 20-24 1994.

[12] R. Volpe, T. Litwin, and L. Matthies. Mobile Robot Localization by Remote Viewing of a Colored Cylinder. In *IEEE/RSJ International Conference on Robots and Systems (IROS)*, Pittsburgh, PA, August 5-9 1995.